Structural Basis for the Binding Affinity of Xanthines with the DNA Intercalator Acridine Orange

Mark B. Lyles,[†] Ivan L. Cameron,*[,†] and H. Ralph Rawls[‡]

Departments of Cellular and Structural Biology, University of Texas Health Science Center at San Antonio, 7703 Floyd Curl Drive, San Antonio, Texas 78229, and Restorative Dentistry, Division of Biomaterials, University of Texas Health Science Center at San Antonio, 7703 Floyd Curl Drive, San Antonio, Texas 78229

Received September 16, 1999

Caffeine (CAF), a methyl-substituted xanthine, interacts with polyaromatic DNA intercalators and has been hypothesized to interfere with their intercalation into DNA. Optical absorption spectroscopy was used to determine the binding affinities (K_{assoc}) and structural effects of a series of methyl-substituted xanthines and a series of methyl-substituted uric acids (8-oxoxanthine) with the known DNA intercalator acridine orange (AO). There is evidence that complexation occurred ($K_{assoc} \geq 150$ M^{-1}; binding curve saturation $\sim \geq 50\%$) between AO and 1,7-dimethylxanthine (155 M^{-1}), 1,3-dimethylxanthine (theophylline, 157 M^{-1}), 1,3,7-trimethylxanthine (CAF, 256 M^{-1}), 1,3-dimethyl-8-chloroxanthine (413 M^{-1}), 1,3,7,9-tetramethyl-8-oxyxanthine (tetramethyl uric acid or TMU, 552 M^{-1}), and theophylline ethylenediamine (aminophylline, 596 M^{-1}). No definitive evidence of complexation occurred between AO and 16 other substituted xanthines or purines, although there was some evidence of weak complexation ($K_{assoc} < 150$ M^{-1}) between AO and eight of the sixteen. Three common structural similarities were identified among those compounds found to form significant bonding with AO: (i) the N_1 or N_3 on the xanthine structure must be substituted with a methyl group; (ii) oxygen or chlorine substitution at C_8 increases binding affinity to AO when resonate states remain unchanged; and (iii) K_{assoc} increases with an increase in number of methyl group substitutions on the 1- or 3-methylxanthine core structure. These results are explained on the basis of complex stabilization due predominately to hydrophobic attraction, with a contribution from charge transfer between donor and acceptor components. This information can be used in the manipulation of the physical or chemical characteristics of biologically active polyaromatic molecules.

Introduction

All known polyaromatic DNA intercalators have the potential to disrupt the normal function of cellular DNA and can lead to mutagenesis, carcinogenesis, and even cell death.[1−3] Many carcinogenic chemicals damage DNA, either in their parent form or after metabolism by cellular enzymes, and for numerous classes of chemicals, the active forms are strong electrophiles.[4−6] Several strategies for the chemoprevention of cancer aim to block this initial DNA damage, either by altering the metabolic pathways away from activation and/or toward detoxification or by "scavenging" the reactive electrophiles.[7,8] Antimutagenic agents that trap or scavenge mutagens and carcinogens have been termed "interceptor molecules" or "desmutagens" and may represent an important first line of defense against carcinogens and mutagens.[8−11]

Review of the literature[6,12−19] suggests that caffeine (CAF), a widely ingested trimethylxanthine, may be able to reduce the cytostatic/cytotoxic activity of agents that share three common properties: (i) they are planar polyaromatic molecules;[1,3,4] (ii) they can interact with double-stranded DNA (dsDNA) via intercalation;[20−24] and (iii) they can form noncovalent complexes with planar polarizing compounds such as CAF.[25−28] When added simultaneously with or immediately before the intercalating agent, CAF has been reported to diminish the cytotoxic effects of the chemotherapeutic drugs doxorubicin (DOX) and novantrone in a variety of cell lines.[14−15] Additionally, CAF reduced the cytotoxicity of the DNA intercalator, ethidium bromide, by reducing its ability to enter cells.[29] The proposed mechanism responsible for the reduction in cytotoxicity by DNA intercalators is the formation of a noncovalent complex between the xanthine and the intercalator.[7,16,17,27,30,31]

This study was conducted to better understand the chemical structures that influence complexation between xanthines and polyaromatic DNA intercalators such as acridine orange (AO). Specifically, experiments were designed to determine the relationship between substitutions on the xanthine core and the resulting K_{assoc} values for complexation with AO. Once the specific structural modification(s) is/are identified, plans call for testing the ability of those xanthines to interfere with intercalation of AO and other polyaromatic mutagens and carcinogens into dsDNA. The specific aims of this first study were to (i) determine the K_{assoc} of various substituted xanthines with AO via spectrophotometric analysis, (ii) compare and contrast the structural differences of various substituted xanthines as they affect K_{assoc}, and (iii) determine if a significant correlation exists between substitutions on the xanthine core structure and K_{assoc} with AO to allow for the prediction

* To whom correspondence should be addressed. Phone, 210-567-3896; e-mail, cameron@uthscsa.edu.
[†] Departments of Cellular and Structural Biology.
[‡] Division of Biomaterials.

10.1021/jm9904708 CCC: $20.00
Published on Web 11/17/2001

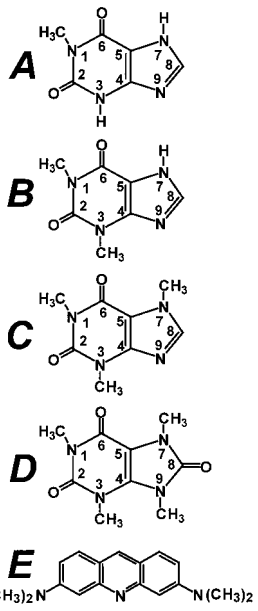

Figure 1. Structural diagrams of the DNA intercalator AO and selective xanthines found to form complexes with AO. Legend: (A) 1-methyl xanthine; (B) 1,3-dimethyl xanthine (theophylline); (C) 1,3,7-trimethyl xanthine (CAF); (D) 1,3,7,9-tetramethyl-8-hydroxy xanthine (tetramethyl uric acid); and (E) 3,6-bis[dimethylamino]acridine (AO).

and/or design of xanthines for the complexation of polycyclic aromatic hydrocarbons (PAHs). It is anticipated that a better understanding of the role of complex formation between intercalating agents such as AO and interceptor molecules such as xanthines will open avenues for practical applications and therapies.

Results

Shifts in the Absorbance Spectrum of AO upon Addition of Increasing Concentrations of Various Modified Xanthines. The spectral shift (red), shown in Figure 2A, in the optical adsorption maximum of AO upon the addition of a particular xanthine, indicates the possibility of a complex being formed between the two compounds. The optical spectrum of AO at 10 μmol is displayed in Figure 2A and exhibits an absorption band in the visible region with a maximum at 495 nm. Upon the addition of 1,3-dimethylxanthine (theophylline), for example, this maximum shifts to 507 nm. This red shift in the absorption maximum of AO in the presence of theophylline provides a convenient method for determining the association constant for the complex formed between AO and theophylline. The optical difference spectrum of the AO−theophylline complex in solution displays a single isobestic point, characteristic of only two absorbing species in solution. The determination of the association constant, K_{assoc}, is determined from the curve in Figure 2C. Using the equation $\Delta A = K(\Delta A_{max})[X]/(1 + K[X])$ (see eq 3, Methods section), the calculated K_{assoc} value for the AO−theophylline complex is 157.0 $\pm$ <0.1 M^{-1}. The other xanthines were similarly analyzed, and their K_{assoc} constants are reported in Table 1.

Of the 22 different xanthines tested, six were determined to have substantial ($\geq$150 M^{-1}) association constants. An additional eight compounds showed some evidence of complex formation with AO. These 14

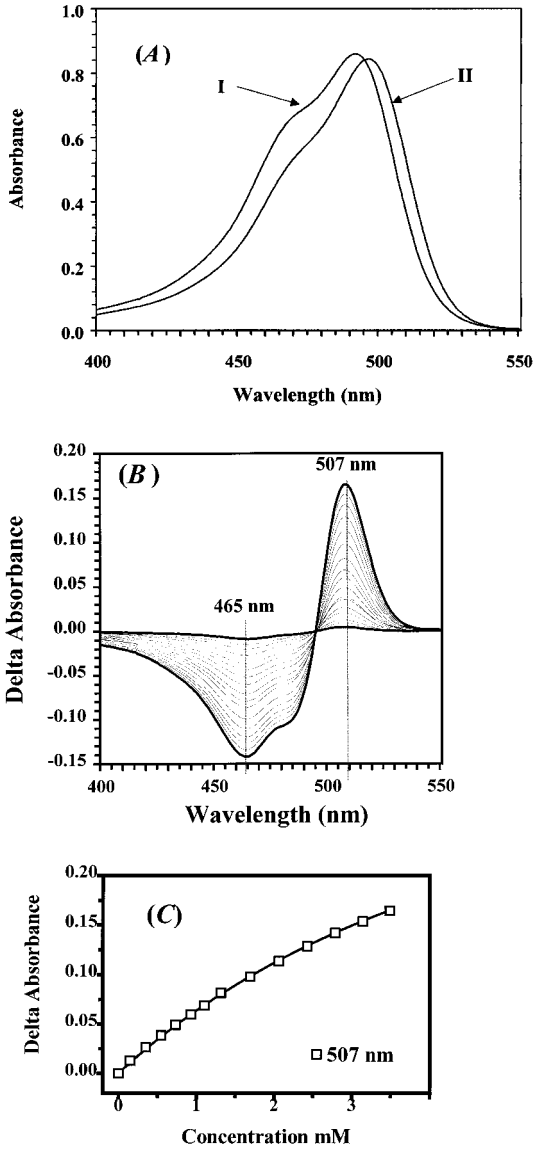

Figure 2. Spectral analysis and K_{assoc} determination for the theophylline−AO complex. (A) Optical absorbance spectra of the theophylline−AO complex in the absence (I) and presence (II) of theophylline. A spectrum of the theophylline−AO complex contains 5 mM of theophylline and 10 μM of AO in solution and has been adjusted for dilution. (B) Absorbance difference spectra of AO titrated with theophylline. Spectral analysis was performed on a series of AO titrations with theophylline. Absorbance values were obtained and adjusted to take into account the effect of dilution. The initial intercalator (AO) concentration was 10 μM in 5 mM HEPES buffer at pH 7.0. Theophylline was pipetted into the AO solution in 1 μL aliquots from a 50 mM stock solution. The resulting plot shows the presence of a single isobestic point, indicative of only two species in solution. (C) The curve used for the determination of the K_{assoc} value between theophylline with AO, as described in the Methods section, is illustrated.

compounds are listed in Table 1 along with the wavelength (nm) at which the binding constant was derived, the concentration range of the xanthine tested (μM), the percent saturation of the binding curve, the K_{assoc} (M^{-1}) value, the regression analysis (R^2) value, the number of resonance states (RS, discussed later), and the number of substituted methyl groups (no. CH_3). None of the seven purines tested revealed any substantial binding affinity with AO.

Table 1. Results of Spectrophotometric Analysis for the Determination of Binding Affinities (K_{assoc}) between AO and Substituted Xanthines (Mean ± SE)

compounds	λ_{max} (nm)	concn (μM)	% satn[b]	K_{assoc} ± SE (M^{-1})	R^2	RS (no. CH_3)
purine	509	25−2199	*[c]	~2	.9914	2 (0)
6-methylpurine		25−805		0		2 (1)
6-chloropurine		10−383		0		2 (0)
1-methyl-6-aminopurine	507	25−1247	*	~14		2 (1)
3-methyl-6-aminopurine	507	25−1507	~7	44.5 ± 0.2	.9996	2 (1)
O-methylguanine (2-amino-6-methoxypurine)	511	25−745	*	~2		4 (1)
guanine monophosphate		50−455		0		4 (0)
xanthine (2,6-dioxypurine)		50−475		0		5 (0)
1-methylxanthine	511	50−536	*	79.2 ± 2.0	.9818	3 (1)
3-methylxanthine	545	50−762	*	~10		4 (1)
7-methylxanthine		25−708		0		4 (1)
1,3-dimethylxanthine (theophylline)	508	248−10 000	61.7	157.0 ± <0.1	1.000	2 (2)
3,7-dimethylxanthine (theobromine)	503	20−412	*	94.5 ± 1.3	.9951	3 (2)
1,7-dimethylxanthine	506	171−10 000	61.7	155.3 ± 3.1	.9956	2 (2)
1,3,7-trimethylxanthine (CAF)	511	495−25 000	86.5	255.7 ± 4.8[d]	.9987	1 (3)
1,3-dimethylxanthine ethylenediamine (aminophylline)	510	25−1503	47.4	596.2 ± 6.5	.9976	1 (4)
uric acid (8-oxyxanthine)		10−338		0		7 (0)
1-methyl-8-oxyxanthine		50−1622		0		5 (1)
7-methyl-8-oxyxanthine		5−305		0		6 (1)
1,3-dimethyl-8-oxyxanthine	509	1000−5000	16.2	38.5 ± 2.2	.9660	4 (2)
1,3-dimethyl-8-chloroxanthine	508	10−5000	67.4	412.5 ± 11.7	.9970	2 (2)
1,3,7,9-tetramethyl-8-oxyxanthine	511	25−1644	47.6	551.5 ± 9.0	.9945	1 (4)

[a] Compounds are grouped on the basis of increasing numbers of carbonyl groups substituted around the purine core structure. The wavelength (λ) in nm of the maximum possible deviation on the delta curve, the square of the correlation coefficient (R^2) of best fit of delta absorbance data (see text for equation), and the concentration range over which the xanthine was analyzed are also shown. A K_{assoc} (M^{-1}) value of zero indicates that no measurable association was detected. The number of resonance states is listed under RS with the number of methyl groups indicated in parentheses at the far right of the table. [b] The percent saturation of the binding curve as calculated by the formula: $K_{assoc}[X]/(1 + K_{assoc}[X]) \times 100$. [c] Percent saturation is less than 10%. [d] As validation of our procedure, the K_{assoc} value of the CAF−AO complex was found to be 256 M^{-1}, which corresponds closely with the value reported by both Larsen et al. (1996) and Kapuscinski and Kimmel (1993) of 258 M^{-1}.

Effect of the Position and Amount of N-Methylation and Electron Affinity of Substituents on Complexation Affinity. Examination of the chemical structure of those compounds that were found to have substantial binding with AO identified three common structural similarities: (i) the N_1 or N_3 on the xanthine core structure must be substituted with a methyl group; (ii) oxygen or chlorine substitution at C_8 increased K_{assoc} when the number of resonance states remained unchanged; and (iii) K_{assoc} increased with an increase in the number of methyl group substitutions, with an excellent empirical fit ($R^2 = 0.99$) to a second-order polynomial equation.

Compounds without methyl group substitution such as xanthine and 8-hydroxyxanthine (uric acid) did not complex with AO, as determined by optical titration. Of the six compounds that exhibited significant K_{assoc} values, all had a methyl group substituted at N_1 and carbonyl groups at C_2 and C_6. Alternatively, compounds without a methyl group at N_1 of the xanthine base structure, but having substituted methyl groups in other positions (3-methylxanthine, 7-methylxanthine, 3,7-dimethylxanthine, and 7-methyl-8-oxyxanthine), showed little or no affinity to complex with AO except for 3,7-dimethylxanthine (theobromine). The compounds 1-methylxanthine, 1-methyl-8-oxyxanthine, 1,3-dimethyl-8-oxyxanthine, and 1,3-dimethyl-8-chloroxanthine have carbonyl groups at C_2 and C_6 and a methyl group substituted at N_1, yet failed to exhibit any significant binding affinity for AO. The only difference between 1-methylxanthine, which has a binding affinity for AO of 79.2 ± 2.0 M^{-1}, and 1-methyl-8-oxyxanthine is a carbonyl group at C_8. Likewise, the only difference between 1,3-dimethylxanthine (theophylline), with a binding constant of 157.0 ± <0.1 M^{-1}, and 1,3-dimethyl-8-chloroxanthine or 1,3-dimethyl-8-oxyxanthine is the presence of an atom with high electron affinity (oxygen or chlorine, respectively) substituted at C_8. The presence of a carbonyl group at C_8 significantly reduces the binding ability of mono- and dimethyl-substituted xanthines except for the tetramethyl-substituted TMU, which exhibits a lower binding affinity than aminophylline, and also contains a total of four methyl groups.

Discussion

The discussion that follows is intended to support the conclusion that the binding of AO to substituted xanthines can be modified by specific R-group substitutions in three systematic ways. The formation of a complex between AO and xanthine derivatives may be predicted based on the theoretical energy state of that particular xanthine. Also discussed is the correlation between the K_{assoc} and the ability of some xanthines to increase solubility of another PAH, benzo[*a*]pyrene, and potential applications of the findings from this study.

Proposed Model for Complex Formation between Xanthines and AO. The solublization capacity (solvent effect) of CAF was first described by Brock and co-workers[38] in 1938 and subsequently detailed by Keilin[39] and Weil-Malherbe.[40] Solubilizing molecules of this type require such factors as planarity, source ionization, and electron-donating properties, which are fulfilled by methylxanthines such as CAF.[42,43] These planar compounds and some derivatives are also able to self-associate in "stacks" in solution[44] as well as intercalate into dsDNA.[45,46]

The ability of substituted xanthines to form molecular complexes with planar polyaromatic hydrocarbons such as AO is controlled to a large extent by the overall energy state of the xanthine molecule.[20,21,47,48] The

energy state of a specific substituted xanthine, the electron-donating molecule, is dependent on five main characteristics: (i) the number of potential resonance states, (ii) the electron-donating or -withdrawing characteristics of the R-group substituents, (iii) the polarity of the R-group substituents, (iv) the degree of steric hindrance by the substituted R-groups, and (v) the physical and chemical characteristics of the solvent system. The characteristics of the solvent system can significantly contribute to complex formation or inhibit it altogether.[48−51] The stabilization of the complex, once formed, depends on the overlap between the highest filled molecular orbital of the donor molecule and the lowest unfilled molecular orbital of the acceptor molecule (AO in the present case). The extent of this overlap depends on the symmetries of these two orbitals and the relative orientations of the molecules.[49]

Additionally, the energy state of the electron-accepting molecule is also significant. In all cases, the formation of a molecular complex must be thermodynamically sound; i.e., in the absence of significant changes in entropy, there must be a reduction in the overall energy states of both molecules for complexation to occur. Specifically, as the energy state of the donor molecule increases, e.g., through R-group substitution, the potential for complexation increases due to the greater stabilization energy available. This explains the observed increase in K_{assoc} values. The relationship between potential resonance states of the xanthine molecule and K_{assoc} suggests that the number of resonance states is a good indicator of the relative energy state of a molecule. Thus, as the number of resonance states increases, the relative energy of the molecule decreases and the driving force for complex formation is reduced. Our results suggest that the formation of a complex between AO and substituted xanthines follows a model first proposed by McKeown et al.[47] where the sandwich-like stacking of two planar molecules forms $\pi-\pi$ interactions. The alternate stacking of polarizing and polarizable molecules (dipole−dipole or dipole-induced dipole) results in van der Waals attraction between the molecules and leads to the formation of stable complexes.[48,50,51]

The hydrophobic effects of the methyl groups are also expected to contribute strongly to the stabilization of the complex through entropic rather than enthalpic phenomena.[52,53] The hydrophobic effects of the methyl groups are due to entropy gain when two hydrophobic molecules form complexes with one another in water, since water molecules are released from their clathrate-like (low entropy) structures about each of the separated hydrophobic molecules, before complex formation.[54,55] Generally, the energy of the excited state is lowered relative to that of the ground state by interactions with solvent molecules, in this case water. The ground state generally has a much smaller dipole moment than the excited state; hence, the solvent stabilization energy is smaller in the ground state than in the excited state, thus leading to a red-shifted absorption spectrum.[56] A similar effect should be relevant due to the interaction of the PAH (AO) molecule in the ground and excited state with the polarizable xanthine molecule.

To elucidate the nature of the stacking interactions, we compared the resulting K_{assoc} values of the xanthine complexes with AO. By forming a complex, the two interacting molecules, i.e., the xanthine and AO, effectively reduce the overall surface area that each molecule exposes to the surrounding water molecules. This leads to the displacement of some water molecules localized near each methyl group and to their inclusion in the general net of hydrogen bonds. Thus, the number of the contacts of methyl groups with water decreases, in agreement with the known hydrophobicity properties of these groups. The observed "protection" of methyl groups of xanthine molecules during stack formation is a typical manifestation of the hydrophobic effect. In the classical case, the stability of the "protected" hydrophobic molecules or groups is caused by the entropy effect.

Although the change in the entropy opposes the association of xanthines and AO, Ts'o et al.[57] proposed the existence of a positive entropy contribution hidden in the general negative entropy value. This contribution may arise from the hydrophobic interaction with the solvent.[58] If hydrophobic interaction between the xanthine molecule and the water results in a more highly ordered structure for the interfacial water, this structured water probably would have a lower entropy than ordinary water. Formation of a stacking complex from the hydrated xanthine accompanied by the decrease in molecular surface area would decrease the amount of ordered water and increase its unitary entropy. Formation of a stacking complex results in a decrease in the amount of ordered water as compared to the hydrated monomers. The association of xanthine and AO molecules leads to the appearance of a water structure that is energetically more preferable around a stack than around monomers. This is the main reason for the stability of stacked complexes in water.

In a study of the fluorescence quenching of human serum albumin by xanthines, Gonzalez-Jimenez and coworkers[59] showed that the quenching mechanism was due to the formation of a xanthine−albumin nonfluorescent complex and that the quenching of the protein fluorescence depends on the number and position of the methyl groups on the xanthines tested. They also reported that the binding process is exothermic and probably hydrophobic with hydrogen bonds playing a significant role in the stabilization of such complexes. Of the three xanthines tested, the fluorescence intensity was quenched by CAF > theobromine > theophylline, implying that the quenching of protein fluorescence depends on the number and position of the methyl groups. It was also reported that the major contributing factor in the stabilization of the complexes is enthalpic rather than entropic in origin. Furthermore, it was suggested that hydrophobic bonds can be involved in the association process because xanthine stays in contact with the tryptophan reside on albumin, which lies in a microenvironment that is essentially hydrophobic, and in this region, fats, drugs, and other hydrophobic materials bind.[60] They suggested that hydrophobic interactions and hydrogen bonding could be the dominant physical forces behind the formation and stabilization of the xanthine−albumin complexes.

Geocintov and co-workers[55] have shown that the covalent binding of the planar PAH benzo[*a*]pyrene diol epoxide (BPDE), with small single-stranded oligonucle-

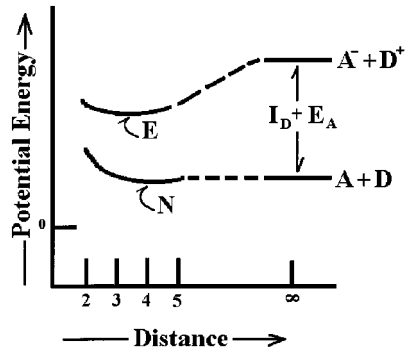

Figure 3. Potential energy curves arising from the resonance of the dative-bond and no-bond electronic states in complexes of xanthines and AO. I_D is the ionization potential of the donor (D; i.e., xanthine), and E_A is the electron affinity of the acceptor (A; i.e., AO). For the ground state, N represents the energy of the complex between A and D (AD), whereas E represents the energy for the excited state. The *X*-axis represents the distance between the two components of the complex A and D, as they approach one another from infinity with relative orientations that are the same as at the equilibrium intermolecular separation (McGlynn, 1958).

otides, is facilitated by hydrophobic binding interactions.[61] These noncovalent interactions, especially the hydrophobic $\pi-\pi$ stacking interactions, are reflected in red shifts in the absorption spectra and diminished molar extinction coefficients of the aromatic pyrenyl residues of BPDE. These data mimic the results from our experiments on the interaction of AO with certain xanthines and further suggest the importance of these interactions on the inhibition of DNA intercalation by mutagens and carcinogens as well as the potential to remove PAH intercalators from DNA.

Theoretical Basis of Electron Donor−Acceptor Interaction. According to McGlynn,[49] complex formation can occur, as depicted in Figure 3, when one molecule acts as an electron donor (D) and another molecule acts as an electron acceptor (A). In this case, the electronic configuration of the ground (lowest energy) states of the separate molecules, A and D, is stabilized by the delocalization provided through the transfer of charge from D to A. This stabilization is the driving force to form the complex. The greater the contribution of the charge transfer state, D^+A^-, to the electronic state of the complex, the greater the stabilization. This stabilization of electronic states is shown in Figure 3, which depicts the potential energy diagram arising from complex formation (taken from McGlynn[49]). Thus, another important factor influencing K_{assoc} in the xanthine−AO complexes may be the extent of resonance stabilization available from the transfer of charge between donor and acceptor.

The first excited state of the complex is stabilized even more than the ground state by charge transfer. Thus, the energy of the transition from the ground state of the complex to the first excited state is decreased, or red-shifted, as compared to the noncomplexed components. This red shift is in turn influenced by any factor that alters the electronic configuration of the donor or acceptor molecules. In the present case, we have studied the influence of substituents on the electronic configuration of xanthine structure (the donor) with AO (the acceptor) by observing the absorption spectra of xanthine−AO complexes.

Relationship between K_{assoc} and N-Methylation, C_8 Substitution, and the Number of Resonance States of the Xanthine Core Molecule. The formation of a complex between any two molecules can only occur when it is thermodynamically advantageous for the complex to exist.[48] Because the formation of a complex allows for a reduction in the overall energy state of a molecule, it would be less thermodynamically advantageous for a lower energy molecule to form a complex than for a higher energy molecule. Thus, as the energy of a molecule decreases, the probability of that molecule forming a complex also decreases. Results from this study suggest that the overall energy state of the xanthine molecule, and therefore its potential to form a complex with AO, is due to three important factors: (i) the number of potential resonance states, (ii) the amount and position of N-methylation, and (iii) the chemical characteristics of the R-group substituted at the C_8 position of the xanthine ring. All of these factors can influence the π-orbital charge distribution, the hydrophobicity of the molecule, the electronic energy state, and, therefore, the thermodynamic potential for the formation of a complex.

Resonance states occur within molecules when, quantum mechanically, they are able to exist simultaneously in different structural forms that delocalize the electronic density. This can occur with a "floating" double bond as seen in the five-membered ring in xanthine or with a double bond that is in equilibrium with a single bond as in tautomeric compounds such as those formed by uric acid. When the resonance states for the molecules tested were counted, those with only one resonance state were found to have the higher K_{assoc} values (see Table 1). Conversely, those molecules with four or more resonance states exhibited little or no complex formation. Examination of the K_{assoc} values for both substituted xanthines and uric acids vs the number of resonance states (Table 1) shows that as the number of resonance states increases, K_{assoc} values decrease significantly. This response can be empirically fitted to a second-order polynomial function ($R^2 = 0.98$). Among the dimethyl-substituted xanthines, 3,7-dimethylxanthine with three potential resonance states has a 41% lower K_{assoc} value than 1,7- or 1,3-dimethylxanthine, both of which have only two potential resonance states. The lower K_{assoc} value for 3,7-dimethylxanthine suggests that there is a lower energy state associated with the higher number of potential resonance states. Both 1,3-dimethylxanthine and 1,7-dimethylxanthine have two potential resonance states and have a similar K_{assoc} value. Structurally, both molecules differ only by the position of the second substituted methyl group on the xanthine core, at either the N_3 or the N_7 position, suggesting that the position of the second methyl substitution contributes little if any to the stability of the complex. Additionally, the difference in K_{assoc} between 1,3-dimethylxanthine and 1,3-dimethyl-8-chloroxanthine, both with only two potential resonance states, must be due to the difference in the chemical characteristics between hydrogen and chlorine. These observations suggest that the number of potential resonance states in which a molecule can exist in addition to the chemical characteristics of the R-group substituents exerts a substantial influence on the energy state of the

xanthine molecule. Consequently, the position of the substitution on the ring structure has only a minor contribution if the number of resonance states is not changed by a shift in the position of the R-group.

A simple way of increasing the electron donor properties of purines or xanthines is N-methylation. The degree to which such methylation increases these properties depends on the chemical structure and, for a given compound, on the position of the alkyl group. On the basis of molecular orbital theory, the position of N-methylation of the xanthine core structure should increase the electron donor properties with $N_3 > N_7 \cong N_9 > N_1$.[62] In uric acid, however, the activation of its electron donor properties should occur for N-methylation at $N_7 > N_3 > N_9 \gg N_1$. As seen in Tables 1 and 2, a pattern of increasing K_{assoc} values between substituted xanthines and AO occurred with increasing N-methylation. With each addition of a methyl group to the xanthine core structure, K_{assoc} approximately doubles. Binding affinity (K_{assoc}) vs methyl group substitution was plotted using the exponential formula $Y = \text{start} \times \exp(K \times X)$, where the plot begins at $Y = \text{start}$ and increases exponentially with rate constant K with a doubling equal to $0.69/K$. Nonlinear regression analysis was also performed and resulted in no significant deviation from the exponential equation ($P = 0.429$) with an R^2 value of 0.99. Thus, a high correlation exists between the number of methyl substitutions on the xanthine ring and the resulting K_{assoc} value.

The results illustrated in Table 1 indicate that binding affinity (K_{assoc}) is also affected by the position of the methylated nitrogens around the xanthine core. Among the monomethylated xanthines, both 1-methylxanthine and 3-methylxanthine were found to exhibit some evidence of weak binding affinity to AO as determined by spectrophotometric analysis, but the binding was not definitive (i.e., $K_{assoc} < 150\ M^{-1}$ and limited concentration range, i.e., saturation < 10%). However, a single methyl substitution at N_7 resulted in no detectable evidence for AO complexation (saturation < 10%). Examination of the xanthine core structure shows that the N_1 position on the ring is situated between two double-bonded oxygen groups, whereas N_3 is near only one double-bonded oxygen at C_2, while N_7 has no double-bonded oxygen nearby. It is proposed that the electron-directing effect of a methyl group enhances the resonance between the lone pair N_7 p orbital electrons and the neighboring oxygen groups. This in turn contributes significantly to the electron density of the π-electron cloud in the vicinity of the ring structure. It is therefore postulated that the contribution to the formation of $\pi-\pi$ bonds between the AO and the monomethyl-substituted xanthines is enhanced by this nearest neighbor effect, with methyl substitution having the greater effect at $N_1 > N_3 > N_7 \cong N_9$. This result suggests that there is some contribution to the stability of the complex due to the elevated energy state of the core molecule through the loss of two resonance states, in addition to the electron donor contribution from the methyl group.

In the case of 1,3-dimethylxanthine ethylenediamine (aminophylline), there are two theophylline groups attached to ethylenediamine. Aminophylline exists in solution as 1,3-dimethyl xanthine (theophylline) bonded ionically at the N_7 position of the xanthine core and the nitrogen at each end of the ethylenediamine linker molecule. The chemical structure of aminophylline in solution can thus best be described as 1,3-dimethylxanthine with an ethylenediamine theophylline R-group ionically bonded at the N_7 position. The resulting K_{assoc} value suggests that the loss of a resonance state, together with the increased electron donor capacity of the R-group at N_7, significantly enhances the ability of theophylline to complex AO by 280% as compared to 63% enhancement with the substitution of a methyl group at N_7 in the case of CAF (1,3,7-trimethylxanthine).

The influence of the number of methyl groups on K_{assoc} is less obvious when there is a simultaneous substitution of either oxygen or chlorine at the C_8 carbon. As can be seen in Table 1, the substitution of a carbonyl group at C_8 significantly decreases the ability of AO to bind with methyl-substituted xanthines (e.g., K_{assoc} for 1,3-dimethyl-8-oxyxanthine is $38.5\ M^{-1}$). By examination of Figure 1, it can be seen that in the xanthine core structure, the double bond at C_8 can resonate between N_7 and N_9 and the hydrogen-substituted carbon at C_8. With a carbonyl substitution at C_8, resonance of the double bond between C_8 and N_7 or N_9 is enhanced and allows for an additional resonate state to exist when the oxygen at C_8 tautamerizes between the carbonyl and the hydroxyl form. Simultaneously, the dipole moment of the molecule has significantly decreased and shifted away from the six-membered ring toward the oxygen at C_8, becoming more centralized over the core structure. With the substitution of chlorine at C_8, the double bond can still resonate between N_7 and N_9, but the π-electron cloud will be less centered above and below the planar rings of the xanthine and, therefore, will be displaced toward the chlorine atom with its higher electron affinity. These features appear to enhance K_{assoc} about 10-fold. It should be noted that the addition of methyl group substitution at N_7 and N_9 tends to offset the electron affinity effects of the carbonyl at C_8 and the resulting change in the dipole moment. Therefore, the substitution of a carbonyl group in the C_8 position creates a mobile or resonate hydrogen (between N_7 and N_9) that is not possible in the trimethylxanthine or the tetramethyl uric acid molecules.

In the case of the AO−CAF system, the spectral change is quite similar to that observed for the AO−DNA intercalation complex,[63] suggesting the occurrence of comparable interaction between the chromophore and the hydrophobic surface of the aromatic compounds such as CAF or DNA base pairs. It is well-known that the monomerizing (disaggregating) capacity of weakly polar solvents, α-cyclodextrin, and detergents originates from the reduction of the degree of dye solvation. This is due to these compounds interposing between the dye molecules and the water molecules.[64,65] Under these conditions, hydrophobic interactions between stacked dye chromophores (dimers) can completely disappear and absorption spectra characteristic of the dye monomers are obtained.

Stockert[66] observed that aromatic cosolutes such a methylxanthines, *o*-phenanthroline, and tannin modify the absorption and emission spectra of dye solutions in a similar way to organic solvents and nucleic acids,[63,67]

Table 2. Relationship between the Number of Methylations on the Xanthine Ring, the K_{assoc} Value with AO (this paper), and the Ability of the Xanthine Compound to Solubilize Benzo(*a*)pyrene in Water as Reported by Weil-Malherbe[40,41]

compounds	CH_3	K_{assoc} (M^{-1})	solubility
1-methylxanthine	1	79[b]	17[c]
1,7-dimethylxanthine	2	155	27
1,3-dimethylxanthine	2	157	28
1,3,7-trimethylxanthine	3	256	100
1,3,7,9-tetramethyl-8-oxyxanthine	4	552	524

[a] Solubility units are based on a comparison to CAF, which was given a value of 100. A nonlinear regression analysis reveals a good fit to the exponential equation $Y = \text{start} \times \exp(K \times X)$ between the number of methyl groups substituted on the xanthine ring and the solubility values reported by Weil-Malherbe[40,41] for xanthines with benzo[*a*]pyrene ($R^2 = 0.98$). A comparison of the results from both the K_{assoc} values and the solubility values from Weil-Malherbe shows a significant linear correlation ($P = 0.002$, $R^2 = 0.90$). [b] Percent saturation of the binding curve was less than 10%. [c] Because of a lack of a specific solubility value for 1-methylxanthine, the average of the solubility values reported for 3-, 7-, and 9-methylxanthine was used.

thus being useful as model systems for the spectral study of dye interactions with cellular substrates.

Cationic dyes with a planar structure such as AO bind to nucleic acids by two different mechanisms: an external interaction with phosphate groups (a metachromatic effect) and the intercalative binding mode in which the dye chromophore is located between two base pairs.[68,69] The corresponding interaction mechanism is based on the occurrence of hydrophobic and dipolar forces between the dye and the hydrogen-bonded purine and pyrimidine bases. Intercalation leads to the isolation of dye monomers within the intercalative sites,[69,70] with the former prevented from interaction with water.[68] Therefore, this hydrophobic binding mode to double-stranded nucleic acids results in a monomerizing effect on the absorption features of the intercalated dye, which is reflected by hypochromic and bathochromic shifts of the main peak.[27,71]

Organic solvents, as well as the internal space of α-cyclodextrin and detergent micelles, provide the same hydrophobic weakly polar environment that occurs in the intercalative cavity of nucleic acids. Likewise, this seems to be the explanation for the monomerizing capacity of aromatic compounds used in this study. In the simplest formulation, hydrophobic interactions between DNA, AO, and planar xanthines can be represented as stacked complexes.

Correlation between the K_{assoc} and the Enhancement of PAH Solubility. Table 2 compares the K_{assoc} values found in Table 1 with the solubility values reported by Weil-Malherbe.[40,41] The effect of structural changes on the interaction of xanthines with AO follows closely those described by Weil-Malherbe in his studies of the solubilization of polyaromatic hydrocarbons with purine bases. The structural differences among a purine, hypoxanthine, xanthine, and uric acid core molecule are the number and presence of oxygen groups bonded to a carbon atom at C_2, C_6, or C_8 of the purine base structure. Purine has no substituted oxygen groups whereas hypoxanthine has an oxygen group substituted at C_6, xanthine has an oxygen at C_2, and C_6, and uric acid has an oxygen at C_2, C_6, and C_8. Weil-Malherbe observed that the solubilization of the PAH benzo[*a*]pyrene increased with increasing N-methylation and, up to a point, with increasing substitutions and increasing electron affinity of the R-groups at C_2, C_6, or C_8 around the purine ring. He found that increasing the number of carbonyl groups around the purine ring increased the solubility of benzo[*a*]pyrene in all cases. However, the substitution of a chloro, thio, or amino group might either increase or decrease solubility. The relationship between N-methylation (*X*-axis) and solubilization (*Y*-axis) can be fitted, empirically, with the exponential equation $Y = \text{start} \times \exp(K \times X)$ ($R^2 = 0.98$). This relationship parallels our results for the relationship between N-methylation and K_{assoc} and further suggests that the solubilization of PAHs such as benzo[*a*]pyrene may be due to complex formation between the PAH and the xanthine and therefore directly related to K_{assoc}. Table 2 compares the K_{assoc} values and the solubility values from Weil-Malherbe[40,41] and reveals the existence of a significant linear correlation ($P = 0.002$, $R^2 = 0.90$) between the two sets of data values. On the basis of these results, solubilization can be used to screen potential interceptor molecules for their ability to form $\pi-\pi$ stacking complexes with DNA. Rapid screening of potential interceptor molecules for their ability to form polarization bonding complexes with DNA intercalators could be achieved using Bowman and Beroza[73−77] partitioning values (P values) utilizing the method described by Robbins.[78]

Potential Applications Based on the Interaction between DNA Intercalators and Xanthines. Polyaromatic hydrocarbons as a class of compounds contain some of the most potent carcinogens as well as some of the most effective antineoplastic drugs. Xanthines, on the other hand, consist of some of the most prevalent plant alkaloids known and are widely ingested on a daily basis. Knowledge of the interaction of selected xanthines with PAHs has practical applications. The interaction of xanthines such as CAF with the antineoplastic drug DOX causes the reduction of blood plasma levels of DOX and a simultaneous increase at the intracellular level.[79,80] The ability to optimize the binding affinity or K_{assoc} value between two interacting classes of compounds would create novel approaches relevant to drug therapy and delivery. For example, enhancing target site concentration of an antineoplastic drug such as DOX could simultaneously increase cellular toxicity while decreasing systemic toxicity.[81] Additionally, interceptor molecules could potentially be designed to bind with specific carcinogens with a very high affinity and therefore significantly reduce their biological effects. Finally, by using the laws of mass action, on which polarization bonding depends, the possibility exists for the creation of compounds for the selective prevention and/or reversal of DNA intercalation by PAHs.

Conclusions

Results from spectral analyses of various xanthines with the DNA intercalator AO demonstrate that specific xanthines can complex with AO. This interaction is attributed to a type of $\pi-\pi$ electron orbital interaction known as polarization bonding. Xanthines with specific R-group substitutions modify binding affinity to AO in three systematic ways: (i) increased with an increase in N-methylation around the xanthine core; (ii) in-

creased by an increase in the potential energy of the xanthine molecule, as evidence by a decrease in the number of resonance states; and (iii) the electron affinity and other chemical characteristics of substitutents affect K_{assoc}. The dominant influence in the formation of such complexes appears to be van der Waals interactions resulting in maximal π-orbital overlap between the two molecules of the complex and the hydrophobic effects of the methyl group substitutions. Additionally, resonance with a donor−acceptor charge transfer state may also contribute to the stabilization of the complex. The hydrophobic effect is an entropic rather than an enthalpic phenomena based on the exclusion of water molecules. These results suggest a possible role for CAF and other xanthines as interceptor molecules in cancer therapy.

We will report separately the results of our chemical studies on the interactions between CAF, AO, and dsDNA and our biological studies with chicken erythrocytes showing the inhibition and reversibility of AO binding to dsDNA.

Materials and Methods

Chemicals and Preparation of Stock Solutions. All xanthines and purines used in this study were obtained commercially at a purity of 98% or greater (Aldrich Chemical Co., Milwaukee, WI) and were used without further purification. Tetramethyl uric acid (1,3,7,9-tetramethyl-8-oxyxanthine) was obtained separately from ICN Biomedicals Inc., Aurora, Ohio. AO (3,6-bis[dimethylamino]acridine hydrochloride), >99% purity, (Aldrich Chemical Co., Milwaukee, WI) was prepared in a stock solution at a concentration of 50 mmol in 5 mmol HEPES buffer (1.0 M solution, Mediatech, Inc., Herndon, VA). AO was chosen as a representative DNA intercalator because of its known spectral characteristics and its wide use as a fluorescence chromophore marker for both DNA and RNA.[32−36] All stock solutions and subsequent dilutions were prepared by dissolving the appropriate weighed amount of compound in 5.0 mmol HEPES adjusted to pH 7.0 with 0.1 M NaOH. Examples of the molecular structure of AO and some selected xanthines found to form complexes with AO are presented in Figure 1.

Choice of Compounds Used in This Study. The compounds used in this study were selected based on their availability, known potential to complex with PAHs, and varying R-group and structural differences. The primary consideration was a purine and/or xanthine base structure with the secondary consideration being *N*-methyl substitution on the base ring structure. Additionally, specific compounds were chosen based on varying R-group substitutions at the C_8 position on the ring structure. This allowed data to be collected to correlate the effect on K_{assoc} of various R-group substitutions based solely on the unique characteristics of that R-group. The effect of increasing the electron affinity on the purine ring was studied by looking at purine, guanine, xanthine, and uric acid. It should be pointed out that the purine core structure has no carbonyl groups. Guanine, which has a carbonyl group at C_6, is indicative of a hypoxanthine core structure. Alternatively, the xanthine core structure has carbonyl groups substituted at C_2 and C_6 on the purine ring, whereas uric acid has carbonyl groups at C_2, C_6, and C_8.

Determination of Complex Formation and K_{assoc} by Absorbance Spectrophotometry. Optical titrations (serial additions of various xanthines to a solution of AO) were performed on a Beckman DU-600 scanning spectrophotometer (Beckman Instrument Co., New York, NY) using a 3 mL (1 cm light path) quartz cuvette containing 2.0 mL of a 10 μmol AO solution. The DU-600 spectrophotometer was blanked with 2 mL of a pH 7.0 buffered 5 mmol HEPES solution over the full range of wavelengths to be scanned prior to sample analysis. This effectively eliminated the need to subtract the background absorbance from the HEPES buffer. Optical absorbance scans were performed over a wavelength range from 400 to 550 nm. No xanthine tested produced absorbance spectra at wavelengths longer than 400 nm. The 10 μmol AO solution was scanned before the start of each titration series to quantitatively monitor any changes in the absorbance spectrum. Optical absorbance experiments were performed using aliquots varying in volume from 1 to 20 μL taken from prepared xanthine stock solutions (5−50 mmol) and titrated into the cuvette containing 2.0 mL of the 10 μmol AO solution. The solution in the cuvette was then thoroughly mixed by 10 s of shaking before scanning. All titrations were performed at room temperature (25 ± 1 °C). The absorbance spectra were measured in 1 nm intervals and stored in digital form. Digitized scan data were converted to a Lotus Spreadsheet file (*.wk1) using a conversion program supplied by the manufacturer (Beckman Instruments, Inc.) and then imported into a Microsoft Excel 97 Workbook file (*.xls) and saved in this format for further analysis. Spectral data for each titration were combined and expressed in graphic form (Excel) (*X*-axis = wavelength in nm; *Y*-axis = optical absorbance) for each xanthine titrated with AO. Initial absorbance data were corrected for the dilution due to the addition of the xanthine by multiplying the absorption value by an adjustment factor determined by the volume of aliquot added.[27] This manipulation slightly increased the absorption value to offset the effects of dilution. Adjusted absorption values were plotted and compared to spectra from noncomplexed AO. This allowed for the visualization of an expected spectral shift that occurs when AO forms a complex with a xanthine.

Determination of Delta Absorbance Values and Delta Plot. When the presence of the xanthine caused a spectral shift, a difference absorbance plot or delta plot was obtained. Delta plots were constructed by subtracting the adjusted absorption spectrum of AO in the presence of the xanthine from the initial spectrum of AO alone at each wavelength and for each aliquot of the titration. This procedure allowed for the creation of difference absorption values or delta absorption values. Delta absorption values obtained in this manner (*Y*-axis = delta absorption) were plotted against wavelength in nanometers (*X*-axis). The appearance of a single isobestic point was indicative of only two species present in solution, AO and an AO complex. Graphic representation allowed for the selection of a wavelength with the maximum sensitivity for determining the association constant. This wavelength was characterized by the greatest positive response in delta absorbance values observed upon addition of each aliquot of xanthine to the AO solution. The AO−xanthine association or binding constant was determined by the following equilibrium expression

$$\mathrm{I} + \mathrm{X} \rightleftharpoons \mathrm{IX} \tag{1}$$

where I represents the intercalator (AO), X represents the interceptor molecule (xanthine), and IX represents the AO−xanthine complex, respectively. This leads to the following equation for the association constant K_{assoc}:

$$\Delta A = KDP_o[\mathrm{X}]/(1 + K[\mathrm{X}])^{37} \tag{2}$$

where ΔA is the change in absorption after addition of a xanthine ($\Delta A \propto [\mathrm{IX}]$) and becomes the *Y*-axis of the delta plot; *D* is the delta extinction coefficient (obtained from a fitted curve, as explained below); [X] is the xanthine concentration (moles) in the cuvette following each aliquot addition; P_o is the concentration of the intercalator (AO) in moles; and *K* is the association constant (K_{assoc}). To solve for *K*, eq 2 thus becomes

$$\Delta A = K(\Delta A_{max})[\mathrm{X}]/(1 + K[\mathrm{X}]) \tag{3}$$

The resulting ΔA values (*Y*-axis = ΔA) were plotted against the final xanthine concentration (*X*-axis = [X]) at the λ_{max} that exhibited the greatest sensitivity for monitoring the formation

of the AO−xanthine complex. The ΔA_{max} value is the maximum absorbance of the complex at saturation (maximum amount of complex that can be formed at equilibrium) and is equivalent to the delta extinction coefficient multiplied by the concentration of substrate (i.e., AO) and can be expressed as $D[P_o]$. The ΔA_{max} value used to calculate the binding association constant (eq 3) was iterated from the initial AO spectrum by two approaches as described below.

Comparison of Binding Affinity (K_{assoc}) between AO and Substituted Xanthines as Determined by Two Different Approaches to Nonlinear Analysis. Equation 3 ($\Delta A = K(\Delta A_{max})[X]/(1+K[X])$) is the binding isotherm for a 1:1 interaction as represented by the binding of AO with xanthines. The experimental data consist of ΔA values obtained as a function of ligand (i.e., xanthine) concentration [X]. The fixed wavelength is chosen to give the largest possible ΔA value. The ΔA_{max} value is the maximum absorbance that can occur when the substrate (AO) is saturated or completely bound to ligand (xanthine). The range of xanthine concentrations [X] analyzed is listed in Table 1 and should ideally cover at least 60% of the binding isotherm or as much as is permitted by the experimental situation (Connors, p 149).[37] Percent saturation is determined using the formula $[K_{assoc}[X]/(1+K_{assoc}[X])] \times 100$. Because of solubility restrictions by many of the xanthines tested, only four compounds exceeded 60% saturation with two compounds at approximately 50% saturation. The ΔA_{max} value used to calculate the binding association constant (eq 3) was iterated from the initial AO spectrum by two approaches.

The first approach to determine K_{assoc} was to select a ΔA_{max} value estimated from the experimental data followed by experimental iteration of this value to maximize the correlation coefficient of the nonlinear analysis (R^2) while not deviating significantly from the model. The second approach for the determination of the K_{assoc} utilized a two parameter fit where both K and ΔA_{max} were allowed to float simultaneously. Results from this second approach yielded mean values with standard error ranges for both K_{assoc} and ΔA_{max}. Comparison of the results between the two approaches indicates that either may be used to determine K_{assoc}, and in all cases, the values obtained for xanthines at approximately 50% saturation and above were not significantly different (data not shown).

Fits to the association curve were determined, and a graph was created by nonlinear least-squares analysis with Prism software (San Diego, CA). The value of the association constant (K_{assoc}) with a standard error was determined from this plot for both approaches described above. (See Connors for a review and discussion of the formulas described above.)[37] Results from the two approaches were compared, and the K_{assoc} values having the highest R^2 values and minimum standard errors are reported in Table 1. In each case where K_{assoc} was determined at xanthine concentrations below approximately 50% saturation of the binding curve, there was evidence to indicate that if $R^2 > 0.99$ then the resulting ΔA_{max} value was a good prediction of the ΔA_{max} value obtained using data taken over a wider concentration range and at xanthine concentrations >50% saturation. The spectra gave evidence for complex formation between an AO and a xanthine even when xanthine concentrations were limited by solubility and the saturation of the binding curve was substantially less than 50%. However, in these cases, a binding constant could only be determined at a low level of confidence; therefore, such values are not given serious weight in the discussion of the results.

As validation of our procedure, the K_{assoc} value of the CAF−AO complex was found to be 256 M^{-1}, which corresponds closely with 258 M^{-1}, the value reported by both Larsen et al.[27] and Kapuscinski and Kimmel.[35]

Acknowledgment. The authors thank Dr. W. E. Hardman and Mr. Jesse Munoz for invaluable help and comments through out all of our work and Dr. G. I. Henderson for kindly allowing us the use of the spectrophotometer. Additional thanks to Drs. M. MacLeod, R. W. Larsen, and N. Geacintov for their helpful and informative discussions and to Dr. G. Adrian and Dr. P. Jagadeeswaran for the reading and comments on earlier drafts of this paper. This work was supported in part by a grant from the National Institute of Dental Research (DE00152).

References

(1) Liquori, A. M.; DeLerma, B.; Ascoli, F.; Transciatti, M. Interaction between DNA and polycyclic aromatic hydrocarbons. *J. Mol. Biol.* **1962**, *5*, 521−526.
(2) Pullman, B. Electronic aspects of the interactions between the carcinogens and possible cellular sites of their activity. *J. Cell. Comp. Physiol.* **1964**, *64* (Suppl. 1), 91−109.
(3) Huberman, E.; Sachs, L.; Yamasaki, H. DNA binding and its relationship to carcinogenesis by different polycyclic hydrocarbons. *Int. J. Cancer.* **1976**, *19*, 122−127.
(4) Miller, E. C.; Miller, J. A. Mechanisms of chemical carcinogenesis. *Cancer* **1981**, *47*, 1055−1064.
(5) Miller, E. C.; Miller, J. A. Searches for ultimate chemical carcinogens and their reactions with cellular macromolecules. *Cancer* **1981**, *47*, 2327−2345.
(6) MacLeod, M. C.; Qing, W. G.; Powell, K. L.; Daylong, A.; Evans, F. E. Reaction of nontoxic, potentially chemopreventive purinethiols with a direct-acting, electrophilic carcinogen, benzo[*a*]pyrene-7, 8-diol 9, 10-epoxide. *Chem. Res. Toxicol.* **1993**, *6*, 159−167.
(7) Dashwood, R.; Guo, D. Antimutagenic potency of chlorophyllin in the Salmonella assay and its correlation with binding constants of mutagen-inhibitor complexes. *Environ. Mol. Mutagen.* **1993**, *22*, 164−171.
(8) Hartman, P. E.; Shankel, D. M. Antimutagens and anticarcinogens: a survey of putative interceptor molecules (published erratum appears in *Environ. Mol. Mutagen.* **1990**, *16* (2), 136). *Environ. Mol. Mutagen.* **1990**, *15*, 145−182.
(9) Ramel, C. Inhibitors of mutagenesis and their relevance to carcinogenesis. *Basic Life Sci.* **1986**, *39*, 511−517.
(10) Ramel, C.; Alekperov, U. K.; Ames, B. N.; Kada, T.; Wattenberg, L. W. International Commission for Protection Against Environmental Mutagens and Carcinogens. ICPEMC Publication No. 12. Inhibitors of mutagenesis and their relevance to carcinogenesis. Report by ICPEMC Expert Group on Antimutagens and Desmutagens. *Mutagen. Res.* **1986**, *168*, 47−65.
(11) Tachino, N.; Guo, D.; Dashwood, W. M.; Yamane, S.; Larsen, R.; Dashwood, R. Mechanisms of the in vitro antimutagenic action of chlorophyllin against benzo[*a*]pyrene: studies of enzyme inhibition, molecular complex formation, and degradation of the ultimate carcinogen. *Mutagen. Res.* **1994**, *308*, 191−203.
(12) Ganapathi, R.; Grabowski, D.; Schmidt, H.; Yen, A.; Iliakis, G. Modulation of adriamycin and *N*-trifluoroacetyladriamycin-14-valerate induced effects on cell cycle traverse and cytotoxicity in P388 mouse leukemia cells by caffeine and the calmodulin inhibitor trifluoperazine. *Cancer Res.* **1986**, *46*, 5553−5557.
(13) Iliakis, G.; Nusse, M.; Ganapathi, R.; Egner, J.; Yen, A. Differential reduction by caffeine of adriamycin induced cell killing and cell cycle delays in Chinese hamster V79 cells. *Int. J. Radiat. Oncol., Biol., Phys.* **1986**, *12*, 1987−1995.
(14) Traganos, F.; Kaminska-Eddy, B.; Darzynkiewicz, Z. Caffeine reverses the cytotoxic and cell kinetic effects of Novantrone (mitoxantrone). *Cell Proliferation* **1991**, *24*, 305−319.
(15) Traganos, F.; Kapuscinski, J.; Darzynkiewicz, Z. Caffeine modulates the effects of DNA-intercalating drugs in vitro: a flow cytometric and spectrophotometric analysis of caffeine interaction with novantrone, doxorubicin, ellipticine, and the doxorubicin analogue AD198. *Cancer Res.* **1991**, *51*, 3682−3689.
(16) Traganos, F.; Kapuscinski, J.; Gong, J.; Ardelt, B.; Darzynkiewicz, R. J.; Darzynkiewicz, Z. Caffeine prevents apoptosis and cell cycle effects induced by camptothecin or topotecan in HL-60 cells. *Cancer Res.* **1993**, *53*, 4613−4618.
(17) MacLeod, M. C.; Mann, K. L.; Thai, G.; Conti, C. J.; Reiners, J. J., Jr. Inhibition by 2,6-dithiopurine and thiopurinol of binding of a benzo[*a*]pyrene diol epoxide to DNA in mouse epidermis and of the initiation phase of two-stage tumorigenesis. *Cancer Res.* **1991**, *51*, 4859−4864.
(18) Shoyab, M. Caffeine inhibits the binding of dimethylbenz[*a*]anthracene to murine epidermal cells DNA in culture. *Arch. Biochem. Biophys.* **1979**, *196*, 307−310.
(19) Rothwell, K. Dose-related inhibition of chemical carcinogenesis in mouse skin by caffeine. *Nature* **1974**, *252*, 69−70.
(20) DeSantis, F.; Giglio, E.; Liquori, A. M. Crystal structure of 1-3-7-9 tetramethyluric acid and the molecular packing in hydromethyl purine crystals. *Nature* **1960**, *188*, 46−48.

(21) DeSantis, F.; Giglio, E.; Liquori, A. M.; Pipamonti, A. Molecular geometry of a 1:1 crystalline complex between 1,3,7,9-tetramethyluric acid and pyrene. *Nature* **1961**, *191*, 900−901.
(22) Van Duuren, B. L. Fluorescence of 1,3,7,9-tetramethyluric acid complexes of aromatic hydrocarbons. *J. Phys. Chem.* **1964**, *68*, 2544−2553.
(23) Booth, J.; Boyland, E. The reaction of the carcinogenic dibenzacarbazoles and dibenzacridines with purines and nucleic acid. *Biochim. Biophys. Acta* **1953**, *12*, 75−87.
(24) MacLeod, M. C. The importance of intercalation in the covalent binding of benzo[*a*]pyrene diol epoxide to DNA. *J. Theor. Biol.* **1990**, *142*, 113−122.
(25) Booth, J.; Boyland, E.; Orr, S. F. D. A spectroscopic study of the nature of the complexes of purines with aromatic compounds. *J. Chem. Soc.* **1954**, 598−603.
(26) Lyles, M. B. Filters for polynuclear aromatic hydrocarbon containing smoke. U. S. Patent 4,517,995, May 14, 1985.
(27) Larsen, R. W.; Jasuja, R.; Hetzler, R. K.; Muraoka, P. T.; Andrada, V. G.; Jameson, D. M. Spectroscopic and molecular modeling studies of caffeine complexes with DNA intercalators. *Biophys J.* **1996**, *70*, 443−452.
(28) Gimenez-Arnau, E.; Missailidis, S.; Stevens, M. F. Antitumour polycyclic acridines. Part 4. Physicochemical studies on the interactions between DNA and novel tetracyclic acridine derivatives. *Anti-Cancer Drug Des.* **1998**, *13*, 431−451.
(29) Boyland, E.; Green, B. The Interaction of Polycyclic Hydrocarbons and Purines. *Br. J. Cancer.* **1962**, *16*, 347−360.
(30) Dashwood, R. H.; Loveland, P. M.; Fong, A. T.; Hendricks, J. D.; Bailey, G. S. Combined in vivo DNA binding and tumor dose-response studies to investigate the molecular dosimetry concept. *Prog. Clin. Biol. Res.* **1990**, *340D*, 335−344.
(31) MacLeod, M. C. Interaction of bulky chemical carcinogens with DNA in chromatin. *Carcinogenesis* **1995**, *16*, 2009−2014.
(32) Robinson, B. H.; Loffler, A.; Schwarz, G. Thermodynamic behavior of acridine orange in solution. Model system for studying stacking and charge effects on self-aggregation. *J. Chem. Soc., Faraday Trans.* **1973**, *69* (1), 56−69.
(33) Kapuscinski, J.; Darzynkiewicz, Z. Interactions of acridine orange with double stranded nucleic acids. Spectral and affinity studies. *J. Biomol. Struct. Dyn.* **1987**, *5*, 127−143.
(34) Kapuscinski, J.; Darzynkiewicz, Z. Spectral properties of fluorochromes used in flow cytometry. *Methods Cell Biol.* **1990**, *33*, 655−669.
(35) Kapuscinski, J.; Kimmel, M. Thermodynamical model of mixed aggregation of intercalators with caffeine in aqueous solution. *Biophys. Chem.* **1993**, *46*, 153−163.
(36) von Tscharner, V.; Schwarz, G. Complex formation of acridine orange with single-stranded polyriboadenylic acid and 5′-AMP: cooperative binding and intercalation between bases. *Biophys. Struct. Mech.* **1979**, *5*, 75−90.
(37) Connors, K. A. *Binding Constants*: *The Measurement of Molecular Complex Stability*; John Wiley & Sons: New York, 1987; pp 75−149.
(38) Brock, N.; Druckrey, H.; Hamperl, H. Zur wirkungsweise cancerogener substanzen. *Biochem. Biophys. Acta* **1938**, *189*, 709−731.
(39) Keilin, J. Effect of caffeine and other imidazole compounds on haematins and their derivatives. *Biochem. J.* **1943**, *37*, 281−289.
(40) Weil-Malherbe, H. The solubilization of polycyclic aromatic hydrocarbons by purines. *Biochem. J.* **1946**, *40*, 351−363.
(41) Weil-Malherbe, H. Effects of purines on fluorescent solutions. *Biochem. J.* **1946**, *40*, 363−368.
(42) Schilt, A. A. Analytical applications of 1,10-phenanthroline and related compounds. *International Series of Monographs in Analytical Chemistry*; Pergamon Press: Oxford, 1969; Vol. 32, pp 193−205.
(43) Kihlman, B. A. *Caffeine and Chromosomes*. Elsevier: Amsterdam, 1997; pp 249−259.
(44) Ishiguro, S.; Wada, H.; Ohtaki, H. Solvation and protonation of 1,10-phenanthroline in aqueous dioxane solutions. *Bull. Chem. Soc. Jpn.* **1985**, *58*, 932−937.
(45) Barton, J. K. Tris (phenanthroline) metal complexes: probes for DNA helicity. *J. Biomol. Struct. Dyn.* **1983**, *1*, 621−632.
(46) Kelly, J. M.; Tossi, A. M.; McConnell, D. J.; Ohuigin, C. A Study of the interactions of some polypyridylruthenium (II) complexes with DNA using fluorescence spectroscopy, topoisomerisation, and thermal denaturation. *Nucleic Acids Res.* **1985**, *13*, 6017−6034.
(47) McKeown, P. J. A.; Ubbelohde, A. R.; Woodward, I. Thermal expansion of *p*-nitroaniline and *p*-dinitrobenzene. *Acta Crystallogr.* **1951**, *4*, 391−395.
(48) Wallwork, S. C. Molecular complexes exhibiting polarization bonding. III. A structural survey of some aromatic complexes. *J. Chem. Soc.* **1961**, 494−499.
(49) McGlynn, S. P. Energetics of molecular complexes. *Chem. Rev.* **1958**, *58*, 1113−1157.
(50) Harding, T. T.; Wallwork, S. C. The structure of molecular compounds exhibiting polarization bonding. I. General introduction and the crystal structure of phenoquinone. *Acta Crystallogr.* **1953**, *6*, 791−796.
(51) Harding, T. T.; Wallwork, S. C. The structure of molecular compounds exhibiting polarization bonding. II. The Crystal structure of the chloranil-hexamethylbenzene complex. *Acta Crystallogr.* **1955**, *8*, 787−794.
(52) Cantor, C. R.; Schimmel, P. R. *Biophysical Chemistry*, *Vol. I*: *The Confirmation of Biological Macormolecules*; Freeman and Sons: San Francisco, CA, 1980.
(53) Cantor, C. R.; Schimmel, P. R. *Biophysical Chemistry*, *Vol. III*: *The Behavior of Biological Macromolecules*; Freeman and Sons: San Francisco CA, 1980.
(54) Shafirovich, V. A.; Courtney, S. H.; Ya, N.; Geacintov, N. E. Proton-coupled photoinduced electron transfer, deuterium isotope effects, and flourescence quenching in noncovalent benzo[*a*]pyrenetetraol nucleoside complexes in aqueous solutions. *J. Am. Chem. Soc.* **1995**, *117*, 4920−4928.
(55) Geacintov, N. E.; Zhao, R.; Kuzmin, V. A.; Kim, S. K.; Pecora, L. J. Mechanisms of quenching of the fluorescence of a benzo[*a*]pyrene tetraol metabolite model compound by 2′ deoxynucleosides. *Photochem. Photobiol.* **1993**, *58* (2), 185−194.
(56) Cantor, C. R.; Schimmel, P. R. *Biophysical Chemistry*, *Vol. II*: *Techniques for the Study of Biological Structure and Function*; Freeman and Sons: San Francisco, CA, 1980.
(57) Ts'o, P. O. P.; Kondo, N. S.; Robins, R. K.; Broom, A. D. *J. Am. Chem. Soc.* **1969**, *91*, 5625−5631.
(58) Kasarda, D. D. Dilution volume changes of some purine and pyrimidine compounds. *Biochem. Biophys. Acta* **1970**, *217*, 535−538.
(59) Gonzalez-Jimenez, J.; Frutos, G.; Cayre, I. Fluorescence quenching of human serum albumin by xanthines. *Biochem. Pharmacol.* **1992**, *44* (4), 824−826.
(60) Walton, A.; Maenpa, F. C. Application of fluorescence spectroscopy to the study of proteins and interfaces. *J. Colloid Interface Sci.* **1979**, *72*, 265−278.
(61) Breslow, R. Hydrophobic effects on simple organic reactions in water. *Acc. Chem. Res.* **1991**, *24*, 159−164.
(62) Pullman, B.; Pullman, A. Electron-donor and -acceptor properties of biologically important purines, pyrimidines, pteridines, flavins, and aromatic amino acids. *Proc. Natl. Acad. Sci. U.S.A.* **1958**, *44*, 1197−1202.
(63) Porumb, II. The solution spectroscopy of drugs and the drug-nucleic acid interactions. *Prog. Biophys. Mol. Biol.* **1978**, *34*, 175−195.
(64) Scott, J. E. Histochemistry of Alcian blue. I. Metachromasia of Alcian blue, Astrablau and other cationic phthalocyanin dyes. *Histochemistry* **1970**, *21*, 277−285.
(65) Juarranz, A.; Stockert, J. C.; Canere, M.; Villanueva, A. A micellar model for the disaggregating effect of detergents on phthalocyanin dyes. *Cell. Mol. Biol.* **1985**, *31*, 379−384.
(66) Stockert, J. C. Cytochemistry of nucleic acids: binding mechanisms of dyes and fluorochromes. *Microsc. Electron. Biol. Cel.* **1985**, *9*, 89−131.
(67) Lober, G.; Schutz, H.; Kleinwachter, V. Effect of organic solvents on the properties of DNA with proflavine and similar compounds. *Biopolymers* **1972**, *11*, 2439−2459.
(68) Lerman, L. S. Acridines mutagens and DNA structure. *J. Cell. Comp. Physiol.* **1964**, *64* (Suppl.), 1−18.
(69) Lerman, L. S. Structural considerations in the interaction of DNA with acridines. *J. Mol. Biol.* **1961**, *3*, 18−30.
(70) Neidle, S.; Berman, H. M. X-ray crystallographic studies of nucleic acids and nucleic acid-drug complexes. *Prog. Biophys. Mol. Biol.* **1983**, *41*, 43−66.
(71) Stockert, J. C. Monomerizing Effect of Caffeine, *o*-phenenthroline, and tannin on cationic dyes: A model system to analyze spectral characteristics of the intercalative binding to nucleic acids. *Acta Histochem.* **1989**, *87*, 33−42.
(72) Pirogov, N.; Shafirovich, V.; Kolbanovskiy, A.; Solntsev, K.; Courtney, S. A.; Amin, S.; Geacintov, N. E. Role of hydrophobic effects in the reaction of a polynuclear aromatic diol epoxide with oligodeoxynucleotides in aqueous solutions. *Chem. Res. Toxicol.* **1998**, *11* (4), 381−388.
(73) Bowman, M. C.; Beroza, M. Identification of pesticides at the nanogram level by extraction p-values. *Anal. Chem.* **1965**, *37*, 291−297.
(74) Bowman, M. C.; Beroza, M. Extraction p-values of pesticides and related compounds in six binary solvent systems. *J. Assoc. Off. Agric. Chem.* **1965**, *48*, 943−950.
(75) Bowman, M. C.; Beroza, M. Extraction of insecticides for cleanup and identification. *J. Assoc. Off. Agric. Chem.* **1965**, *48*, 358−366.

(76) Bowman, M. C.; Beroza, M. Identification of compounds by extraction p-values using gas chromatography. *Anal. Chem.* **1966**, *38*, 1544−1549.
(77) Bowman, M. C.; Beroza, M. Device and method for determining extraction p-values with unequilibrated solvents or unequal phase volumes. *Anal. Chem.* **1966**, *38*, 1427−1431.
(78) Robbins, W. K. *Polynuclear Aromatic Hydrocarbons*: *Chemistry and Biological Effects*; Battelle Press: Columbus, OH, 1979; pp 841−853.
(79) Sadzuka, Y.; Iwazaki, A.; Miyagishima, A.; Nozawa, Y.; Hirota, S. Effects of methylxanthine derivatives on adriamycin concentration and antitumor activity. *Jpn. J. Cancer Res.* **1995**, *86* (6), 594−599.
(80) Hosenpud, P.; Wright, J.; Simpson, L.; Abramson, J. Caffeine enhances doxorubicin cardiac toxicity in an animal model. *J. Card. Failure* **1995**, *1* (2), 155−160.
(81) Sadzuka, Y.; Iwazaki, A.; Sugiyama, T.; Sawanishi, H.; Miyamoto, K. 1-methyl-3-propyl-7-butylxanthine, a novel biochemical modulator, enhances therapeutic efficacy of adriamycin. *Jpn. J. Cancer Res.* **1998**, *89* (2), 228−233.
(82) Sadzuka, Y.; Egawa, Y.; Sugiyama, T.; Sawanishi, H.; Miyamoto, K.; Sonobe, T. Effects of 1-methyl-3-propyl-7-butylxanthine (MPBX) on Idarubicin-induced antitumor activity and bone marrow suppression. *Jpn. J. Cancer Res.* **2000**, *91* (6), 655−657.

JM9904708